Archives of Microbiology (2023) 205:163
https://doi.org/10.1007/s00203-023-03507-x

ORIGINAL PAPER

Overexpression of putative glutathione peroxidase from *Neopyropia*-associated microorganisms in *Chlamydomonas* to respond to abiotic stress

Jeong Hyeon Kim[1] · Eun-Jeong Park[2] · Jong-il Choi[1]

Received: 9 January 2023 / Revised: 10 March 2023 / Accepted: 22 March 2023 / Published online: 3 April 2023

Abstract
Lipid accumulation in microalgae can be substantially enhanced by exposing the microalgae to abiotic stress, thus increasing biofuel production. However, this also generates reactive oxygen species (ROS), which disrupts cell metabolism and reduces their productivity. Previous mRNA sequencing analyses in *Neopyropia yezoensis* and its associated microorganisms elucidated a putative glutathione peroxidase (PuGPx) gene. Here, this putative glutathione peroxidase was overexpressed in the microalga *Chlamydomonas reinhardtii*, which increased cell growth and survival rates compared to the control group under abiotic stress. Additionally, increased lipid accumulation was observed under salinity stress, high-temperature stress, and hydrogen peroxide (H_2O_2)-induced oxidative stress. These results suggest that PuGPx plays a protective role against abiotic stress in *C. reinhardtii* and stimulates lipid accumulation, which could be considered advantageous in terms of biofuel production.

Keywords Abiotic stress · *Chlamydomonas reinhardtii* · Lipid accumulation · Putative glutathione peroxidase · Survival rate

Introduction

With the exacerbation of climate change caused by the burning of fossil fuels, energy production from biomass has recently garnered increasing attention. Microalgae are currently being studied as potential third-generation, industrial-grade biomass. Compared to existing plant-based biomass sources, microalgae have unique advantages in terms of photosynthetic efficiency, the ability to grow more efficiently in polluted environments, and the ability to fix carbon dioxide, all of which align with global sustainable development goals (Ahorsu et al. 2018; Dębowski et al. 2020). Microalgae accumulate various neutral lipids such as triacylglycerol in their cells, which can be used as biodiesel after undergoing transesterification (Hu et al. 2008; Klok et al. 2014). When microalgae undergo abiotic stress (e.g., nutrient, temperature, and salinity stress), large quantities of lipids accumulate in their cells for survival and maintenance. However, these abiotic stressors can also induce oxidative stress, which reduces the growth rate of microalgae and lowers their overall productivity, thus increasing the cost of biofuel production (Bibi et al. 2022; Paliwal et al. 2017; Rodolfi et al. 2009). Therefore, developing abiotic stress-resistant microalgae is essential to increase lipid production.

Red algae have traditionally been used in food and medicine, particularly in East Asian countries such as China, Japan, and Korea. *Neopyropia* is a genus of red algae (Yang et al. 2020) that grows in environments characterised by large temperature differences, osmotic stress, and strong light levels (Lee et al. 2018; Park and Choi 2020; Rezayian et al. 2019). Several studies have sought to identify the molecular mechanisms through which *Neopyropia* responds to abiotic stress. A previous study demonstrated that heterologous introduction of the putative ACSMD (2-amino-3-carboxymuconate-6-semialdehyde decarboxylase) gene from

Communicated by Yusuf Akhter.

✉ Eun-Jeong Park
ejpark74@korea.kr

✉ Jong-il Choi
choiji01@jnu.ac.kr

[1] Department of Biotechnology and Bioengineering, Chonnam National University, Gwangju 61186, Republic of Korea

[2] Aquatic Plant Variety Center, National Institute of Fisheries Science, Mokpo 58746, Republic of Korea

N. yezoensis into *Chlamydomonas reinhardtii* increased its tolerance to low nitrogen levels (Park et al. 2022). Recent mRNA sequencing analyses of *Neopyropia yezoensis* elucidated some interesting genes from microorganisms attached to *Neopyropia* (hereinafter referred to as *Neopyropia*-associated microorganisms) (Park and Choi 2020). Among them, glutathione peroxidase (GPx) is an antioxidant enzyme that protects the cell from reactive oxygen species (ROS)-induced lipid peroxidation, protein oxidation, and DNA oxidation. Glutathione peroxidase is widely known to respond to abiotic stress and has been characterised in many plants. Seaweeds are known to produce a variety of bioactive compounds, including GPx, which are important for their survival in harsh marine environments. However, to the best of our knowledge, no previous studies have characterised the glutathione peroxidase gene from *Neopyropia* sp. and *Neopyropia*-associated microorganisms. Studying GPx from avariety of organisms is of great interest due to the potential benefits it may offer.

Based on the above-described observations, this study sought to examine the cellular changes induced by the insertion of PuGPx from *Neopyropia*-associated microorganisms into *C. reinhardtii*, after which we characterised the responses of the recombinant *C. reinhardtii* to abiotic stressors such as high salinity, high temperature, and direct oxidative stress.

Materials and methods

Strains and growth conditions

E. coli DH5α (RBC Bioscience, New Taipei, Taiwan) was used as a gene cloning host, whereas *C. reinhardtii* cc-125 was used to evaluate the effects of PuGPx expression on the growth profile and lipid accumulation. The *C. reinhardtii* cells were incubated in Tris–acetate-phosphate (TAP) medium and cultured at 25 ℃ while being shaken at 150 rpm under a continuous cool white light (40 µmol protons m^{-2} s^{-1}). The TAP medium consisted of 2.42 g/L Tris-base, 25 mL/L TAP-salts (Beijerinck salts; 15 g/L ammonium chloride [NH_4Cl], 4 g/L magnesium sulphate heptahydrate [$MgSO4{\cdot}7H_2O$], and 2 g/L calcium chloride dehydrate [$CaCl_2{\cdot}2H_2O$]), 1 mL/L phosphate solution (288 g/L dipotassium hydrogen phosphate [K_2HPO_4] and 144 g/L potassium dihydrogen phosphate [KH_2PO_4]), 1 mL/L acetic acid, and 1 mL/L Hutner's trace elements solution. The Hutner's trace metal solution contained 50 g/L ethylenediaminetetraacetic acid disodium salt dehydrate [$Na_2EDTA{\cdot}2H_2O$], 22 g/L zinc sulphate heptahydrate [$ZnSO_4{\cdot}7H_2O$], 11.4 g/L boric acid [H_3BO_3], 5 g/L manganese chloride tetrahydrate [$MnCl_2{\cdot}4H_2O$], 5 g/L ferrous sulphate heptahydrate [$FeSO_4{\cdot}7H_2O$], 1.6 g/L cobalt chloride hexahydrate [$CoCl_2{\cdot}H_2O$], 1.6 g/L copper sulphate pentahydrate [$CuSO_4{\cdot}H_2O$], and 1.1 g/L diammonium molybdate [$(NH_{4)6}MoO_3$].

Table 1 Primers used in this study

Primer	Primer sequence	Target gene
GPx-F	ATCCCATGGATGAAGAAGGTGATC GGGA	PuGPx amplification, qRT-PCR
GPx-R	ATCGATATCTTAGTAGTTCTTCTG GCA	
tubA-F	CTC GCT TCG CTT TGA CGG TG	*Tubulin A*, internal control for qRT-PCR
tubA-R	CGT GGT ACG CCT TCT CGG C	

Multiple sequence alignments

The DNA sequence and the amino acid sequence of PuGPx from *Neopyropia*-associated microorganisms were obtained from previous reports (Park and Choi 2020). PuGPx was found not to belong to the *Neopyropia* genome. This amino acid sequence was compared with those of other bacteria including Bacteroidia (MBP7261321.1), Sphingomonadales (MBM3920284.1), Flavobacteriaceae (MBK5209038.1), Chitinophagaceae (MCF8292247.1), and Lewinellaceae (MCB9313222.1) using the Cluster Omega software (version 1.2.2).

Vector construction and transformation

The PuGPx DNA sequence for expression was designed according to the codon usage of the host, *C. reinhardtii* (Watts et al. 2021). Specific primers were based on this sequence and fabricated for cloning (Table 1). These contained the restriction enzyme sites of *Nco*I and *Hind*III. DNA fragments corresponding to PuGPx were amplified by a polymerase chain reaction (PCR) using the GPx-F and GPx-R primers. Plasmid pCr102 was used as a vector for this study (Kim et al. 2011). pCr102_PuGPx was constructed by inserting PuGPx DNA fragments obtained by digestion with *Nco*I and *Hind*III after PCR. For transformation, the cells were incubated in TAP media for three days once the cells reached the mid-log phase (3.0×10^6 cells/mL). Cells were centrifuged at 2,500 rpm for 5 min and resuspended in TAP medium containing 60 mM of sucrose (TAP-60 mM sucrose).

For each cell sample (250 µL), 1 µg of DNA was mixed in a Gene Pulser Cuvette (Bio-Rad, CA, USA), after which the

samples were incubated for 5 min at 16 ℃. Electroporation was conducted at 750 V, 25 µF, and 200 Ω of resistance. After electroporation, the cells were incubated for 10 min at room temperature. The cells were recovered by transferring them to TAP-60 mM sucrose and incubating for one day while being shaken at 200 rpm under white light. The transgenic lines were selected by incubating the cells on TAP agar media containing hygromycin B (50 µg/mL).

RNA isolation

Mid-log phase cells were centrifuged at 12,000 rpm for 5 min and resuspended with 1 mL Trizol® LS Reagent (Ambion, Inc., Austin, TX). The samples were then mixed for 10 min by vortexing, incubated at room temperature for 5 min, and centrifuged at 13,000 rpm for 10 min at 4 ℃. After separating the supernatant, 250 µL of chloroform (Duksan Pure Chemical Co., Ansan, Republic of Korea) was added, mixed by vortexing for 2 min, and centrifuged for 10 min at 4 ℃. The supernatant was mixed for 2 min after the addition of an equal volume of phenol–chloroform (50:50 v/v; Ambion Inc.) and centrifuged. The supernatant was then mixed with an equal volume of isopropanol (Daejung Chemical Co., Siheung, Republic of Korea) and stored at 4 ℃ for 1 h. The mixture was centrifuged for a further 20 min and the precipitated RNA pellet was washed with 70% ethanol (v/v). The RNA pellet was dried at room temperature for 5–7 min and resuspended in diethylpyrocarbonate water.

Quantitative real-time PCR (qRT-PCR)

Quantitative real-time PCR (qRT-PCR) was performed to confirm whether the cells were transformed and to observe any changes in expression levels. cDNA was synthesised using a first-strand cDNA synthesis kit (Takara Bio Inc., Kusatsu, Japan) following the manufacturer's instructions. The primers used for qRT-PCR are summarised in Table 1. The qRT-PCR analyses were conducted using TB green premix Ex Taq (Takara) coupled with a real-time PCR system (Illumina Inc., San Diego, CA). The reaction consisted of 40 cycles of 95 ℃ for 10 s followed by 58 ℃ for 30 s. The data were analysed using the $2^{-\Delta\Delta Ct}$ method (Livak and Schmittgen 2001) and *Tubulin A* was used as the internal control to calculate relative gene expression.

Measurement of survival rate and growth profile under abiotic stress

To examine the cell survival rate under saline and oxidative stress, agar plates were prepared with 0, 100, 200, and 300 mM sodium chloride (NaCl) or 0, 5 and 10 mM hydrogen peroxide (H_2O_2), respectively. The *C. reinhardtii* harbouring pCr102 (Cr_pCr102) and recombinant *C. reinhardtii* overexpressing PuGPx (Cr_PuGPx) were cultured for three days, after which they were washed with 1 × phosphate-buffered saline. Next, 10 µL of cells were spotted onto the plates described above. Cell survival rates were determined by measuring colony numbers in the non-saline or non-H_2O_2-TAP plate and comparing them with the cells in the TAP plates containing different saline or H_2O_2 concentrations.

High-temperature stress was evaluated as described in a previous study (Hema et al. 2007). Cells were initially exposed to a gradual increase in temperature [30 ℃ (2 h) + 35 ℃ (1 h)], after which they were exposed to 40 ℃ for 1 h or 2 h, followed by 42 ℃ for 1 h or 2 h. Finally, the cells were washed with 1 × phosphate-buffered saline and 10 µL of cells were spotted onto the TAP plates. The cells were then cultured at 25 ℃ under cool white light for six days and the survival rates were calculated as described previously.

To measure the growth profile under oxidative stress, the cells were cultured for three days, and 0, 0.1, or 0.5 mM H_2O_2 was added to the culture medium. The same procedure was used to measure the growth profile under saline-stress conditions, but 100, 200, or 300 mM NaCl was instead added to the culture medium. The same conditions were employed when measuring the profile under high-temperature conditions. Optical density was measured daily over the three-day culture period at 750 nm using a UV spectrophotometer (Molecular Devices, San Jose, CA).

Microscopic observations and quantification of lipid droplets

Nile red (Sigma-Aldrich, MO, USA) was used to stain the cells, as this allows for the identification of lipid droplets through fluorescence microscopy (Carl Zeiss, Oberkochen, Germany). After dissolving the staining reagent in 5% acetone (5 µg/ml), the cells were incubated in the dark for 30 min at 37 ℃ (Cirulis et al. 2012). Lipids were quantified as described in a previous study (Park et al. 2022).

Results

Analysis of sequence alignment of PuGPx from *Neopyropia*-associated microorganisms

The amino acid sequence of the PuGPx taken from *Neopyropia*-associated microorganisms overexpressed in *C. reinhardtii* was compared with those of other species (Fig. 1). Levels of conservation of 58.59%, 54.21%, 63.64%, 57.63%,

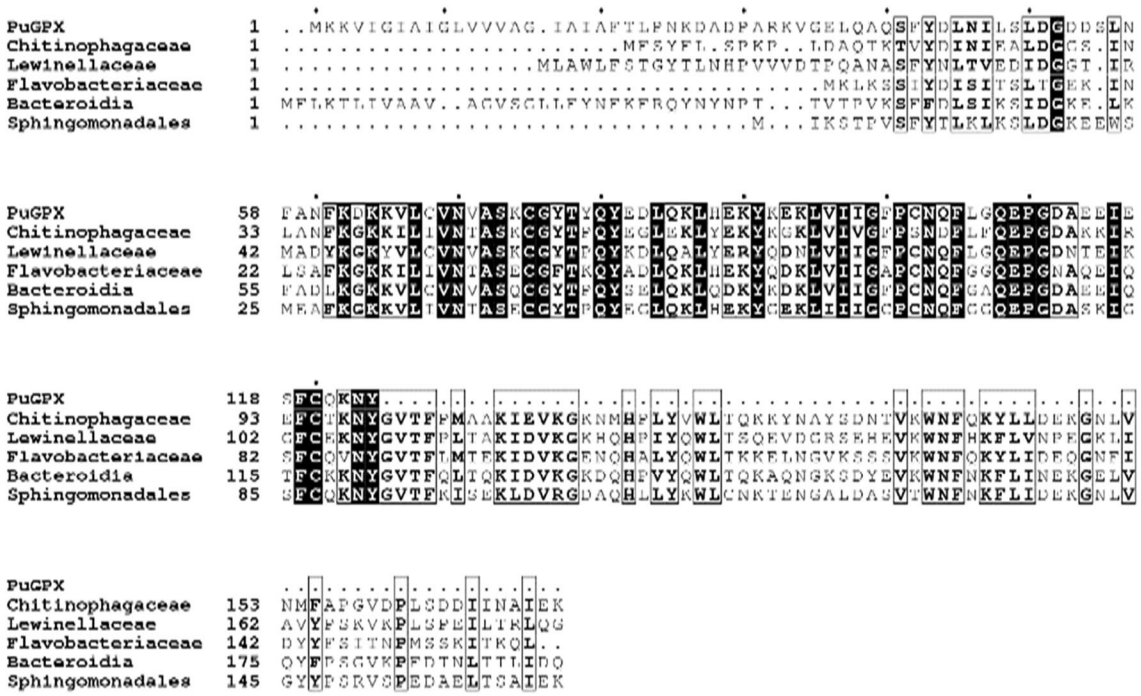

Fig. 1 Multiple sequence analysis of putative glutathione peroxidase from *N. yezoensis*-associated microorganisms for *C. reinhardtii* and other representative species: Bacteroidia (MBP7261321.1), Sphingomonadales (MBM3920284.1), Flavobacteriaceae (MBK5209038.1), Chitinophagaceae (MCF8292247.1), and Lewinellaceae (MCB9313222.1)

and 64.84% were observed relative to bacteria belonging to different taxa, including Chitinophagaceae, Lewinellaceae, Flavobacteriaceae, Bacteroidia, and Sphingomonadales, respectively. From the alignment results, the PuGPx from *Neopyropia*-associated microorganisms was found to possess conserved regions for GPx in other species and could therefore be functionally expressed in *C. reinhardtii.*

Construction of recombinant *C. reinhardtii* overexpressing PuGPx and comparison of the cell growth profile, survival rate, and lipid accumulation under abiotic stress

qRT-PCR was used to select a recombinant strain in which pCr102-PuGPx was inserted for overexpressing the PuGPx gene (Fig. 2). Upon comparing the gene expression levels of the control group (Cr_pCr102) and the recombinant cells (Cr_PuPGx), our findings confirmed that Cr_PuGPx had a five-fold higher expression of PuGPx relative to *Tubulin A* (internal control).

Saline stress conditions

Cell growth profiles were measured to confirm the resistance of the recombinant strain under saline-stress conditions.

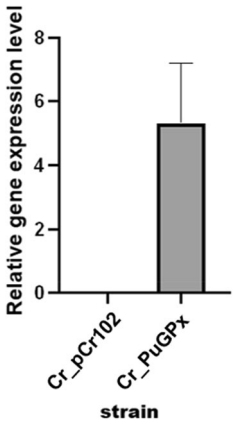

Fig. 2 Determinations of PuGPx transcript levels in PuGPx transgenic lines (Cr_PuGPx). Data are expressed as mean ± standard deviation, n = 3

Under the 100 mM NaCl conditions, the final cell density increased by 5% in Cr_PuGPx compared with the Cr_pCr102, whereas cell density increased by 6% under the 300 mM NaCl conditions (data not shown). In contrast, a 1.26-fold increase in final cell density was observed in Cr_PuGPx under the 200 mM NaCl conditions (Fig. 3a).

The survival rates under saline-stress conditions were also calculated (Fig. 3b). Cr_pCr102 and Cr_PuGPx exhibited survival rates of 40.9% and 52.0% under the 100 mM NaCl condition, 14.1%, and 32.4% under the 200 mM NaCl

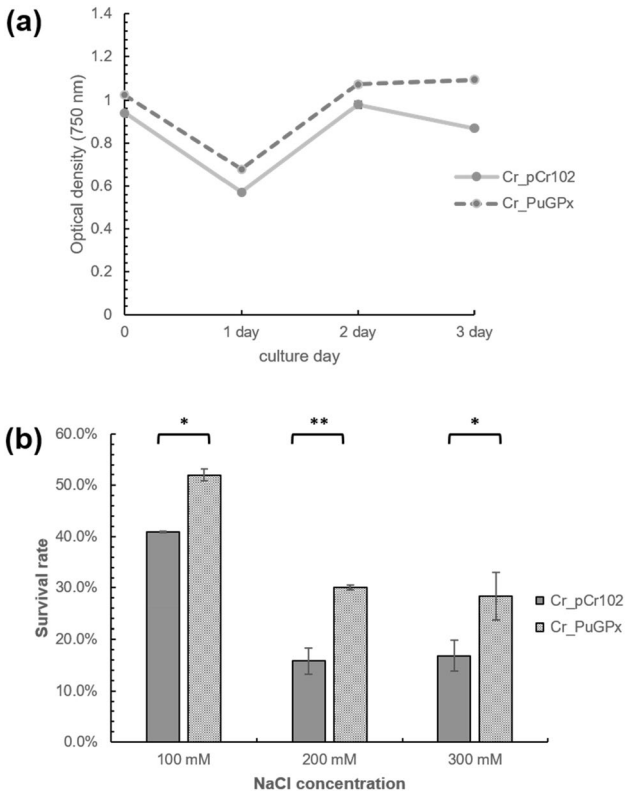

Fig. 3 Comparison of Cr_PuGPx and Cr_pCr102 cells under saline-stress conditions. (a) Growth profiles in 200 mM NaCl-TAP medium for three days. (b) Survival rates in TAP agar plate containing 100, 200 and 300 mM NaCl, respectively. Data are expressed as the mean ± standard deviation; n = 3; statistical analysis was carried out using Student's *t*-tests. *$p < 0.05$, **$p < 0.005$

condition, and 15.2% and 31.3% under the 300 mM NaCl condition, respectively. When comparing the two strains under the three aforementioned conditions, the survival rates of Cr_PuGPx increased by 1.27, 2.29, and 1.87, respectively.

Qualitative and quantitative confirmation was also carried out to compare the lipid accumulation of Cr_pCr102 and Cr_PuGPx under saline-stress conditions (Fig. 4). On Day 1, in the 100 mM NaCl condition, the lipid contents of Cr_PuGPx and Cr_pCr102 were 2.76% and 1.33%, respectively; in the 200 mM NaCl condition, the lipid contents were 4.72% and 2.98%; and in the 300 mM NaCl condition, the lipid contents were 8.68% and 2.62%. In other words, Cr_PuGPx exhibited a 2.08-, 1.58-, and 3.31-fold increase in accumulated lipid droplets compared to Cr_pCr102 under each of the tested conditions. On Day 3, the lipid contents Cr_PuGPx and Cr_pCr102 were 1.67% and 1.93% under the 100 mM NaCl condition; 12.78% and 1.31% under the 200 mM NaCl condition; and 7.44% and 3.14% under the 300 mM NaCl condition. The decease of lipid accumulation in Cr_PuGPx was not statistically significant under the 100 mM NaCl condition. Overall, our findings indicated that lipid accumulation in Cr_PuGPx increased 9.79 times under the 200 mM NaCl condition and 2.36 times under the 300 mM NaCl condition.

High-temperature stress conditions

To determine stress tolerance at high temperatures, growth profile, survival rate, and lipid accumulation were observed after the cells had been incubated for 1 h and 2 h at 40 °C and 42 ℃. Cell growth profiles after recovering from high-temperature stresses were measured once a day for three days. Compared with the final optical densities of Cr_pCr102 after 1 h and 2 h of incubation at 40 ℃, Cr_PuGPx showed an increase of 14% and 20%, respectively (Fig. 5a, b). When incubated at 42 ℃, the cell density of Cr_PuGPx was higher than that of Cr_pCr102 on the 2nd day. However, its final cell density decreased by 2% and 5% after 1 and 2 h of incubation, respectively (data not shown).

The survival rate was measured by counting the number of colonies recovered from the general TAP medium after the cells were exposed to heat stress. The survival rates for Cr_pCr102 and Cr_PuGPx were 60.0% and 92.9% after 1 h incubation, 14.3% and 149.5% after 2 h at 40 ℃, 50.0% and 132.4% after 1 h at 42 ℃, and 91.0% and 189.8% after 2 h at 42 ℃. These results demonstrated that the survival rates of Cr_PuGPx were 1.55, 10.45, 2.64, and 2.08 times greater than those of Cr_pCr102 under each of the aforementioned conditions.

Microscopic observation coupled with qualitative and quantitative analysis of lipid droplet accumulation was performed once a day in cells exposed to high-temperature conditions (Fig. 6). Our findings indicated that, after 1 day, the lipid contents in Cr_pCr102 and Cr_PuGPx were 1.52% and 1.02% when incubated at 40 ℃ for 1 h. In contrast, the lipid contents were 0.51% and 2.62% when the cells were incubated at 40 ℃ for 2 h, respectively. When incubated at 42 ℃ for 1 and 2 h, the lipid contents of Cr_pCr102 and Cr_PuGPx were 0.4% and 2.47%, and 0.72% and 3.67%, respectively. Cr_PuGPx exhibited higher lipid accumulation under most conditions, except when incubated at 40 ℃ for 1 h, showing 5.18-, 6.15-, and 5.12-fold differences under conditions 40 ℃ for 2 h, 42 ℃ for 1 h, and 42 ℃ for 2 h, respectively. After three days of incubation at 40 ℃ for 1 h, Cr_pCr102 and Cr_PuGPx exhibited lipid contents of 0.65% and 4.92%, respectively, whereas the cells incubated at 40 ℃ for 2 h exhibited lipid contents of 2.00% and 6.93%. The Cr_pCr102 samples incubated at 42 ℃ for 1 h exhibited a 2.95% lipid content, whereas the Cr_PuGPx samples incubated at 42 ℃ for 1 h exhibited lipid contents of 3.51%. The Cr_pCr102 samples had a 1.12% lipid content, whereas the Cr_PuGPx samples

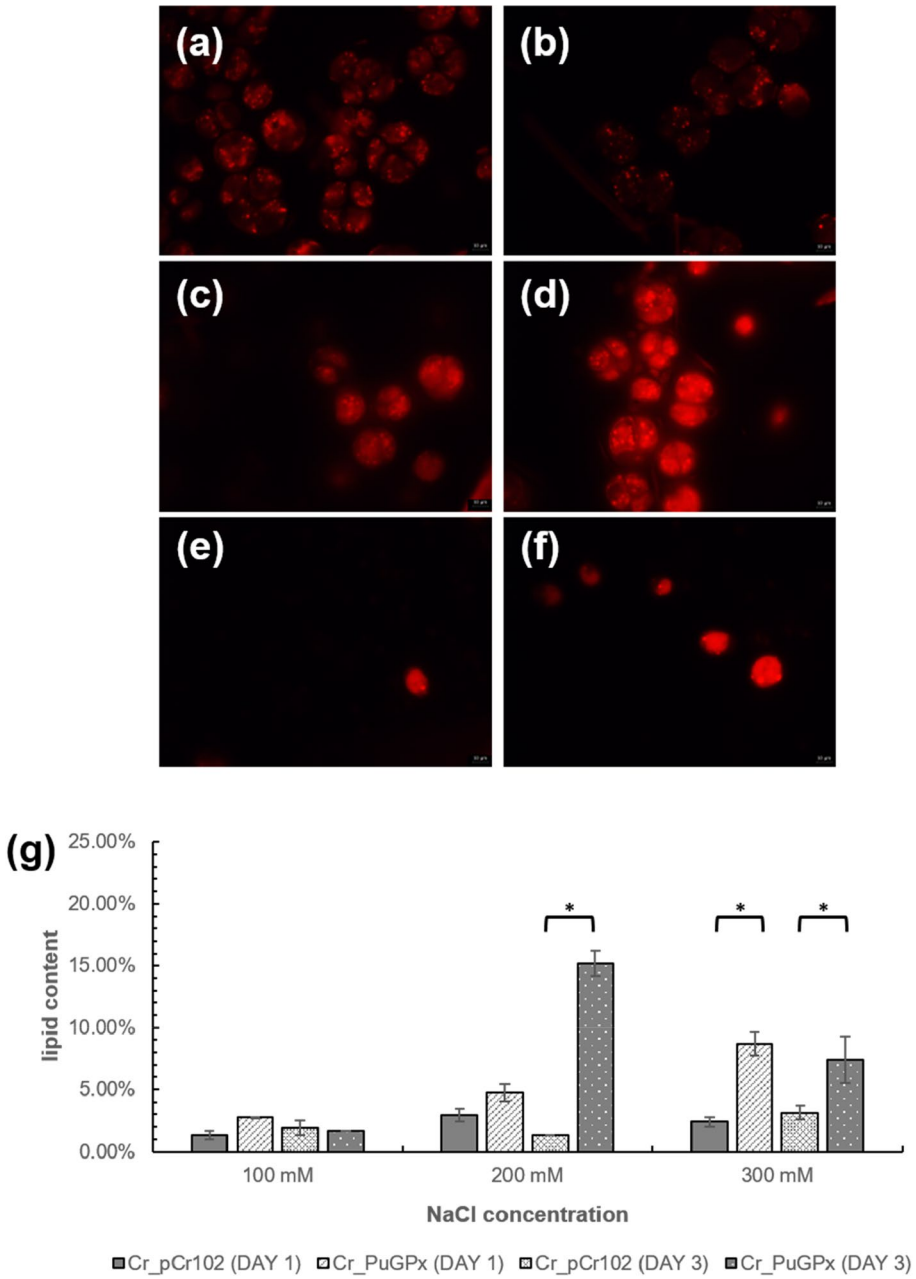

Fig. 4 Nile red-stained microscopic images and quantitative analysis of lipids in Cr_pCr102 (**a**, **c**, **e**) and Cr_PuGPx (**b**, **d**, **f**) under NaCl stress. **a**, **b** Under 100 mM NaCl, **c**, **d** under 200 mM NaCl, **e**, **f** under 300 mM NaCl for 3 days, **g** The quantitative data for lipid content. Data are expressed as the mean ± standard deviation; n = 3; statistical analysis was carried out using Student's *t*-tests. *$p < 0.05$. Scale bar = 10 μm

incubated at 42 ℃ for 2 h had lipid contents of 5.55% when incubated at 42 ℃ for 2 h.

After three days of culturing, the lipid content tended to increase compared to the 1st day in all Cr_PuGPx and Cr_pCr102 samples except for the Cr_pCr102 sample incubated at 40 ℃ for 1 h. Cr_PuGPx exhibited 7.56-, 1.19-, 1.19-, and 4.95-fold increases in lipid content for each condition (40 ℃ for 1 h, 40 ℃ for 2 h, 42 ℃ for 1 h, and 42 ℃ for 2 h, respectively) compared with the control group.

Hydrogen peroxide stress conditions

Abiotic stress induces ROS production (You and Chan 2015). Therefore, to confirm the resistance of cells to ROS, oxidative stress was applied with various concentrations of H_2O_2, and cell growth profiles, survival rates, and lipid accumulation were subsequently observed. Under the 0.1 and 0.5 mM H_2O_2 conditions, the final cell densities of Cr_PuGPx after three days of culture were similar to or slightly lower than those of Cr_pCr102. However, the optical densities of the Cr_PuGPx cells were 13.3% and 16.8% higher

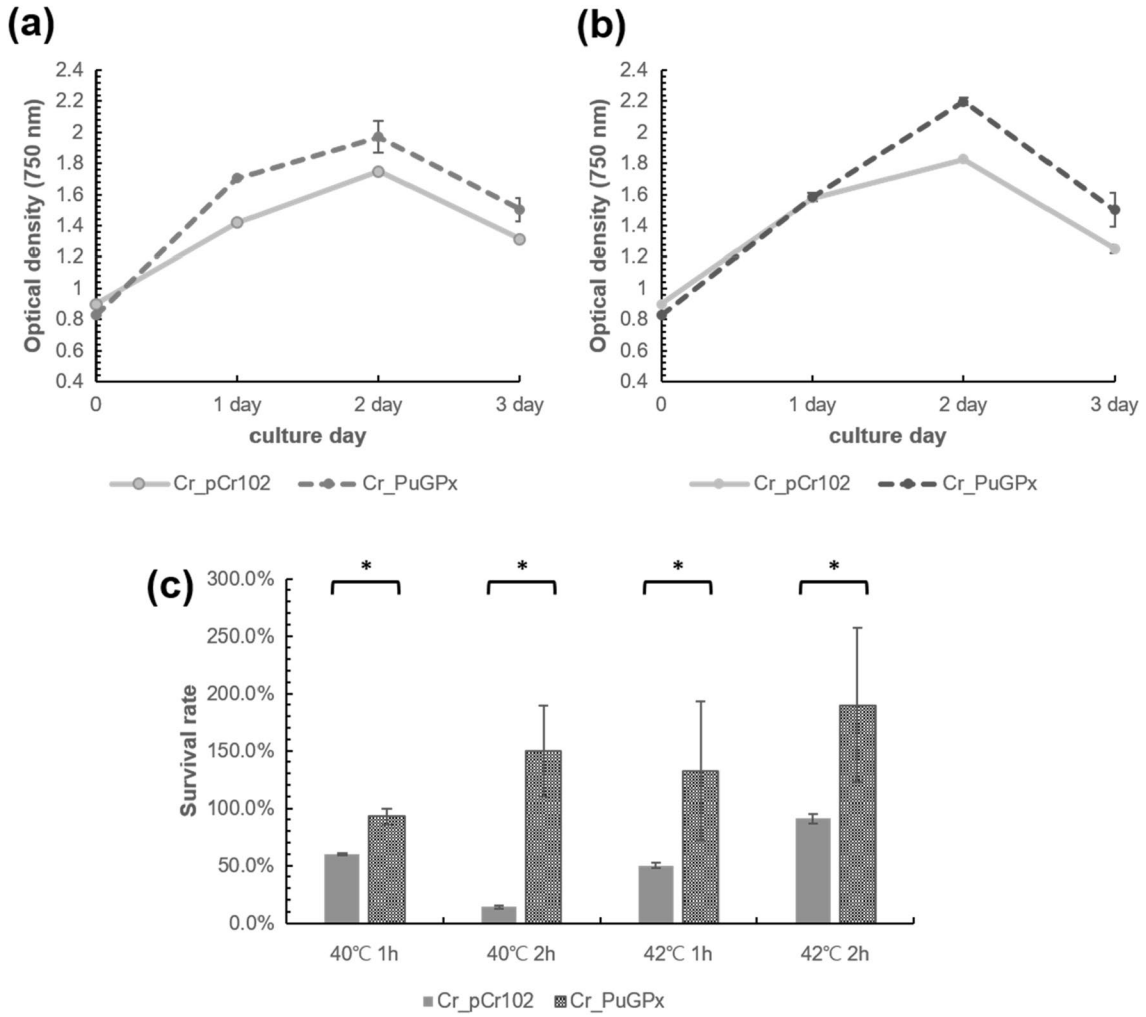

Fig. 5 Comparison of Cr_PuGPx and Cr_pCr102 cells under high-temperature stress conditions. **a** Growth profiles during recovery after 1 h incubation at 40 ℃. **b** Growth profiles during recovery after 2 h incubation at 40 ℃. **c** Survival rates under various high-temperature stresses. Data are expressed as the mean ± standard deviation; n = 3; statistical analysis was carried out using Student's *t*-tests. **p* < 0.05

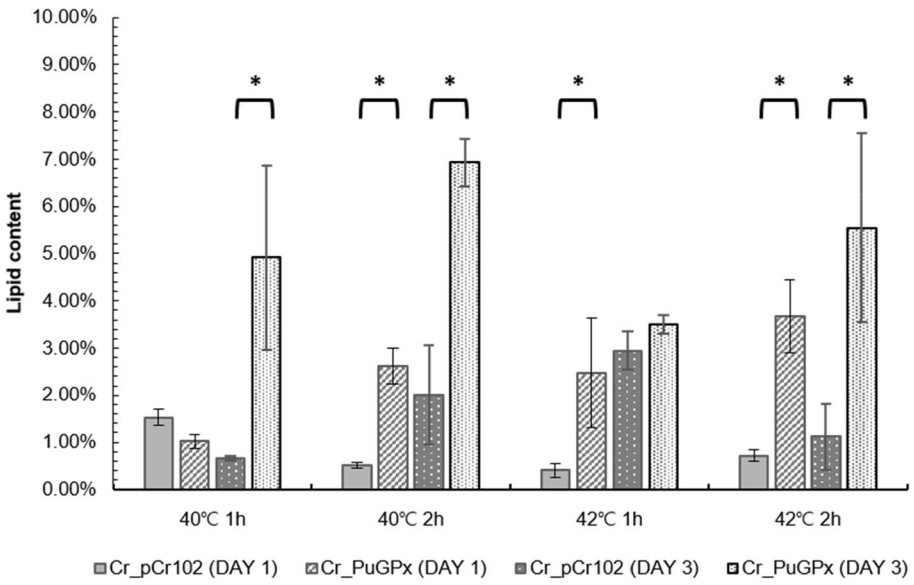

Fig. 6 Quantitative analysis of lipids accumulations in Cr_PuGPx and Cr_pCr102 under high-temperature stress. Data are expressed as the mean ± standard deviation; n = 3; statistical analysis was carried out using Student's *t*-tests. **p* < 0.05. Scale bar = 10 µm

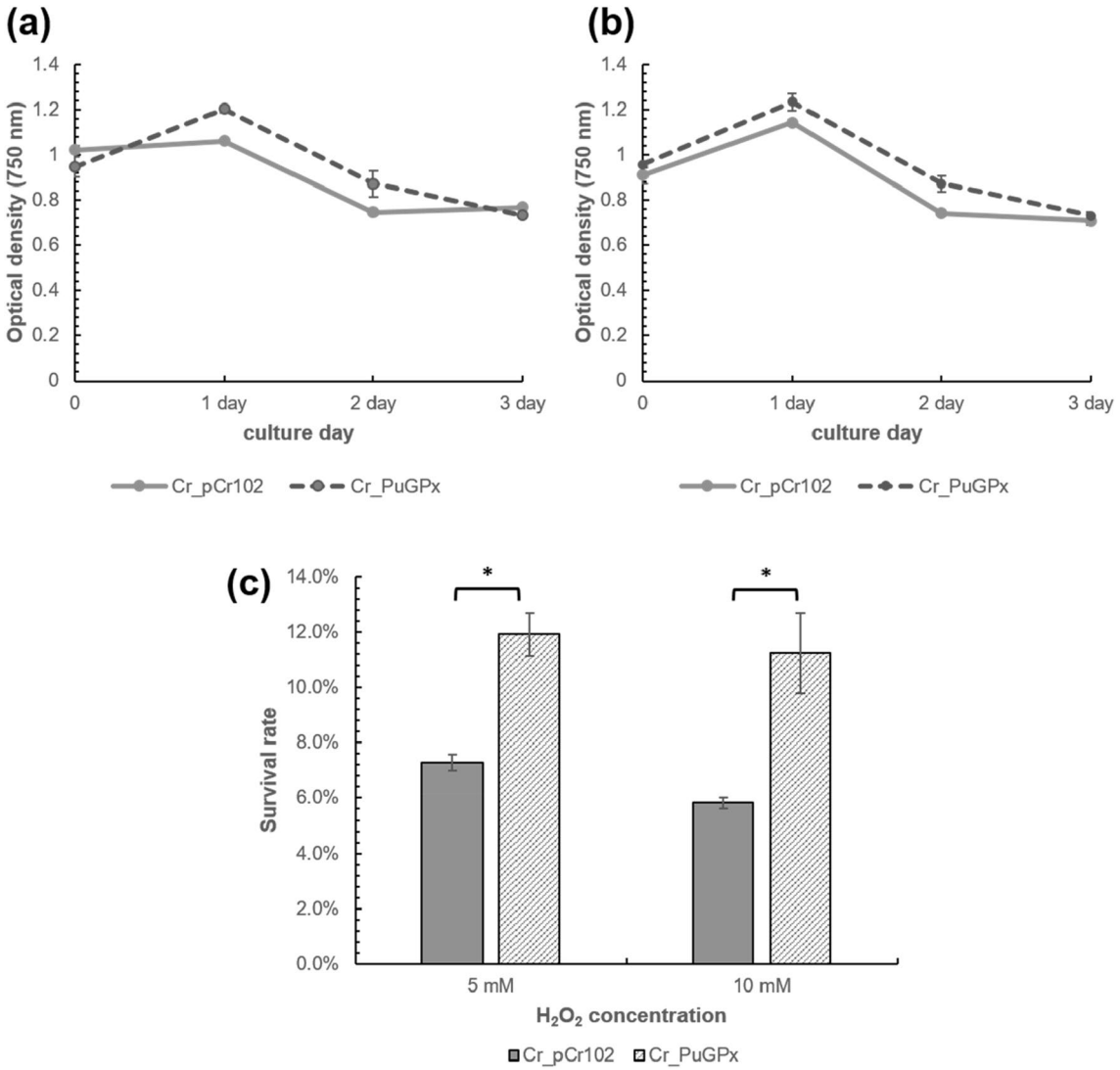

Fig. 7 Comparison of Cr_PuGPx and Cr_pCr102 cells under H_2O_2 conditions. **a** Growth profiles in 0.1 H_2O_2-TAP medium, and **b** 0.5 mM H_2O_2-TAP medium for 3 days. **c** Survival rates in TAP agar plate containing 5,10 mM H_2O_2. Data are expressed as the mean ± standard deviation; n = 3; statistical analysis was carried out using Student's *t*-tests. *$p < 0.05$

than those of Cr_pCr102 after one and two days of culturing under the 0.1 mM H_2O_2 condition, respectively, whereas they increased by 7.9% and 17.4% under the 0.5 mM H_2O_2 condition, respectively (Fig. 7a, b).

The Cr_pCr102 and Cr_PuGPx cells exhibited survival rates of 7.3% and 11.9% in 5 mM H_2O_2 and 5.8% and 11.2% in 10 mM H_2O_2 (Fig. 7c). When comparing these two strains, the results indicated that Cr_PuGPx exhibits a 1.63-fold increase in survival rates under the 5 mM H_2O_2 condition and a 1.93-fold increase under the 10 mM condition (Fig. 7c).

Microscopic observation after Nile red staining showed that the lipid content of Cr_pCr102 and Cr_PuGPx were almost identical under the 0.1 mM H_2O_2 condition after one day of culturing, with values of 1.25% and 1.19%, respectively (Fig. 8). An approximately 1.54-fold difference was observed under the 0.5 mM H_2O_2 condition, with values of 1.55% and 2.39%, respectively. After three days of culturing, a 4.73-fold difference was observed between the samples under the 0.1 mM H_2O_2 condition, with values of 2.15% and 10.17% respectively, whereas a 6.51-fold difference was observed under the 0.5 mM H_2O_2 condition, with values of 1.34% and 8.72%, respectively.

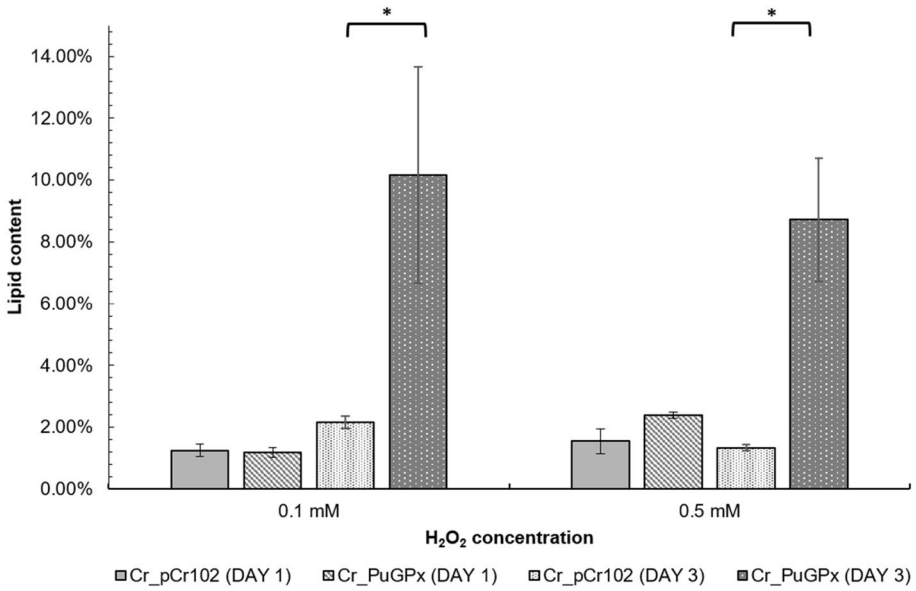

Fig. 8 Quantitative analysis of lipid accumulations in Cr_PuGPx and Cr_pCr102 and under oxidative stress. Data are expressed as the mean ± standard deviation; n = 3; statistical analysis was carried out using Student's *t*-tests. $*p < 0.05$

Discussion

ROS such as hydrogen peroxide (H_2O_2), singlet oxygen (O_2^-), and hydroxyl radicals (OH^-) reduce growth and photosynthesis rates and also cause DNA damage (Lee et al. 2018; Rezayian et al. 2019). In previous studies, the overexpression of the antioxidant enzymes ascorbate peroxidase (APX) and superoxide dismutase (SOD) derived from *N. yezoensis* in *C. reinhardtii* resulted in higher growth rates compared to the control group under oxidative stress and salinity stress (Lee et al. 2018). GPx, a similar antioxidant enzyme, reduces excess H_2O_2 to H_2O and O_2 using reduced glutathione (GSH) as an electron donor (Yu et al. 2020). When comparing the sequence of the PuGPx gene with that of other related species, it was found that it shared more than 40% sequence identities (Fig. 1), meaning that they are likely to share functional similarities (Pearson 2013). These results suggest that recombinant *Chlamydomonas* overexpressing PuGPx is more tolerant to abiotic stress.

Plants and algae are most commonly exposed to salinity stress and high-temperature stress. The induction of thermal stress is expected to be cost-effective because it reduces the cost of cooling treatment (Béchet et al. 2017). Additionally, this approach can be effectively applied to outdoor photoreactors used for microalgal biomass production (Gupta et al. 2019). The expression of PuGPx in *C. reinhardtii* conferred resistance to abiotic stress and direct oxidative stress in microalgae. Furthermore, lipid accumulation was also increased by over expression of PuGPx.

Glutathione peroxidase (GPx) (EC 1.11.1.9) belongs to an enzyme family with peroxidase activity, whose main biological role is to protect living organisms from oxidative damage. Specifically, the biochemical function of glutathione peroxidase is to reduce lipid hydroperoxides to their corresponding alcohols and to reduce free hydrogen peroxide to water. Therefore, the overexpression of GPx in *Chlamydomonas* can increase the growth rate and survival rates when challenged with abiotic stress. Our findings indicated that Cr_PuGPx had higher lipid accumulation rates compared to the control group. This was likely because *C. reinhardtii* can obtain carbon by fixing CO_2 through photosynthesis and synthesising lipids while resisting oxidative stress (Lee et al. 2018; Wase et al. 2014). Given that GPx overexpression is an indicator of abiotic stress resistance, a similar reaction is expected to occur in response to oxidative stress during the photosynthesis of lipids. Therefore, our findings demonstrated that resistance to abiotic stress could promote biofuel production using microalgae by stimulating lipid production.

Author contributions EJP and YC designed the study and carried out the sample collection. JHK carried out experiments and conducted the data analysis and wrote the final version of the manuscript. All authors read and approved the final version of the manuscript.

Funding This work was supported by a National Research Foundation of Korea (NRF) grant funded by the Korean government (MSIT) (NRF-2018R1D1A1B07049359) and the National Institute of Fisheries Science, Ministry of Oceans and Fisheries, Korea (R2023022).

Data Availability Sequences will be available under the following NCBI GenBank accession numbers: Bacteroidia (MBP7261321.1), Sphingomonadales (MBM3920284.1), Flavobacteriaceae (MBK5209038.1), Chitinophagaceae (MCF8292247.1), and Lewinellaceae (MCB9313222.1).

Declarations

Competing interests The authors declare no competing interests.

Consent to participate The study has not involved any human or animal participation or data.

Consent for publication All authors gave their consent for publication.

References

Ahorsu R, Medina F, Constantí M (2018) Significance and challenges of biomass as a suitable feedstock for bioenergy and biochemical production: a review. Energies 11(12):3366. https://doi.org/10.3390/en11123366

Béchet Q, Laviale M, Arsapin N, Bonnefond H, Bernard O (2017) Modeling the impact of high temperatures on microalgal viability and photosynthetic activity. Biotechnol Biofuels 10:1–11

Bibi F, Jamal A, Huang Z, Urynowicz M, IshtiaqAli M (2022) Advancement and role of abiotic stresses in microalgae biorefinery with a focus on lipid production. Fuel 316:123192. https://doi.org/10.1016/j.fuel.2022.123192

Cirulis JT, Strasser BC, Scott JA, Ross GM (2012) Optimization of staining conditions for microalgae with three lipophilic dyes to reduce precipitation and fluorescence variability. Cytometry A 81A(7):618–626. https://doi.org/10.1002/cyto.a.22066

Dębowski M, Zieliński M, Kazimierowicz J, Kujawska N, Talbierz S (2020) Microalgae cultivation technologies as an opportunity for bioenergetic system development—advantages and limitations. Sustainability 12(23):9980. https://doi.org/10.3390/su12239980

Gupta S, Pawar SB, Pandey R, Kanade GS, Lokhande SK (2019) Outdoor microalgae cultivation in airlift photobioreactor at high irradiance and temperature conditions: effect of batch and fed-batch strategies, photoinhibition, and temperature stress. Bioprocess Biosyst Eng 42:331–344

Hema R, Senthil-Kumar M, Shivakumar S, Chandrasekhara Reddy P, Udayakumar M (2007) *Chlamydomonas reinhardtii*, a model system for functional validation of abiotic stress responsive genes. Planta 226(3):655–670

Hu Q, Sommerfeld M, Jarvis E, Ghirardi M, Posewitz M, Seibert M, Darzins A (2008) Microalgal triacylglycerols as feedstocks for biofuel production: perspectives and advances. Plant J 54(4):621–639

Kim E, Park HS, Jung Y, Choi DW, Jeong WJ, Park HS, Hwang MS, Park EJ, Gong YG (2011) Identification of the high-temperature response genes from *Porphyra seriata* (rhodophyta) expression sequence tags and enhancement of heat tolerance of *Chlamydomonas* (chlorophyta) by expression of the porphyra htr2 gene1. J Phycol 47(4):821–828. https://doi.org/10.1111/j.1529-8817.2011.01008.x

Klok A, Lamers P, Martens D, Draaisma R, Wijffels R (2014) Edible oils from microalgae: insights in TAG accumulation. Trends Biotechnol 32(10):521–528

Lee HJ, Yang HY, Choi JI (2018) Study of functional verification to abiotic stress through antioxidant gene transformation of *Pyropia yezoensis* (Bangiales, Rhodophyta) APX and MnSOD in *Chlamydomonas*. J Microbiol Biotechnol 28(7):1217–1224. https://doi.org/10.4014/jmb.1802.02024

Livak KJ, Schmittgen TD (2001) Analysis of relative gene expression data using real-time quantitative PCR and the $2^{-\Delta\Delta CT}$ method. Methods 25(4):402–408. https://doi.org/10.1006/meth.2001.1262

Paliwal C, Mitra M, Bhayani K, Bharadwaj SV, Ghosh T, Dubey S, Mishra S (2017) Abiotic stresses as tools for metabolites in microalgae. Biores Technol 244:1216–1226

Park SJ, Choi JI (2020) De novo transcriptome analysis of high growth rate *Pyropia yezoensis* (Bangiales, Rhodophyta) mutant with high utilization of nitrogen. Acta Bot Croat 79(2):201–2011

Park SJ, Ahn JW, Choi JI (2022) Improved tolerance of recombinant *Chlamydomonas rainhardtii* with putative 2-amino-3-carboxymuconate-6-semialdehyde decarboxylase from *Pyropia yezoensis* to nitrogen starvation. J Microbiol 60(1):63–69. https://doi.org/10.1007/s12275-022-1491-7

Pearson WR (2013) An introduction to sequence similarity ("homology") searching. Curr Protoc Bioinformatics. https://doi.org/10.1002/0471250953.bi0301s42

Rezayian M, Niknam V, Ebrahimzadeh H (2019) Oxidative damage and antioxidative system in algae. Toxicol Rep 6:1309–1313

Rodolfi L, ChiniZittelli G, Bassi N, Padovani G, Biondi N, Bonini G, Tredici MR (2009) Microalgae for oil: Strain selection, induction of lipid synthesis and outdoor mass cultivation in a low-cost photobioreactor. Biotechnol Bioeng 102(1):100–112

Wase N, Black PN, Stanley BA, DiRusso CC (2014) Integrated quantitative analysis of nitrogen stress response in *Chlamydomonas reinhardtii* using metabolite and protein profiling. J Proteome Res 13(3):1373–1396

Watts A, Sankaranarayanan S, Watts A, Raipuria RK (2021) Optimizing protein expression in heterologous system: Strategies and tools. Meta Gene 29:100899. https://doi.org/10.1016/j.mgene.2021.100899

Yang LE, Deng YY, Xu GP, Russell S, Lu QQ, Brodie J (2020) Redefining Pyropia (Bangiales, Rhodophyta): four new genera, resurrection of Porphyrella and description of *Calidia pseudolobata* sp. nov. from China. J Phycol 56(4):862–879

You J, Chan Z (2015) ROS regulation during abiotic stress responses in crop plants. Front Plant Sci 6:1092

Yu B, Yang J, Niu J, Wang G (2020) Antioxidant responses to hyperosmolarity stress in the intertidal *Pyropia yezoensis* (Bangiales, Rhodophyta). Algal Res 48:101930. https://doi.org/10.1016/j.algal.2020.101930